Supporting Information

Adsorption in Purely Dispersive Systems from Molecular Simulation, Density Gradient Theory, and Density Functional Theory

Jinlu Liu,[†] Michaela Heier,[‡] Walter G. Chapman,[†] and Kai Langenbach[*,‡]

[†]*Department of Chemical and Biomolecular Engineering, Rice University, 6100 Main St, Houston,Texas, 77005, USA*

[‡]*Laboratory of Engineering Thermodynamics(LTD), Technische Universität Kaiserslautern, Erwin-Schrödinger-Str. 44, 67663 Kaiserslautern, Germany*

E-mail: kai.langenbach@mv.uni-kl.de

A. States for fitting φ via the radial distribution function $g(r^*)$

All bulk states used for fitting φ with the resulting pressure of the Perturbed Truncated and Shifted (PeTS) equation of state (EOS) and the self-consistent density functional theory (DFT1) as well as the resulting adjustable parameter φ are given in Table 1.

Table S1: Parameter φ and bulk fluid pressure p_f^* predicted with PeTS EOS and DFT1 for changing temperature T^* and bulk fluid density $\rho_\mathrm{f}^{*\mathrm{b}}$.

T^*/T_c^*	$\rho_\mathrm{f}^{*\mathrm{b}}$	p_f^* (PeTS EOS)	p_f^* (DFT1)	φ
0.7	0.0026	0.0025506	0.0025519	1.21
	0.0078	0.0073587	0.0073635	1.21
	0.0130	0.011784	0.011775	1.21
	0.76	0.044700	0.046400	1.00
	0.77	0.15830	0.13970	0.99
	0.78	0.28467	0.25674	0.98
	0.79	0.42463	0.43738	0.98
	0.80	0.57890	0.58478	0.97
	0.81	0.74825	0.74775	0.96
	0.82	0.93342	0.92714	0.95
	0.83	1.1352	1.1238	0.94
0.8	0.0067	0.0064434	0.0064509	1.21
	0.0200	0.017755	0.017759	1.21
	0.0334	0.027261	0.027068	1.21
	0.69	0.024700	0.013700	1.03
	0.70	0.081300	0.091600	1.03
	0.71	0.14552	0.14815	1.02
	0.72	0.21806	0.21278	1.01
	0.73	0.29949	0.28620	1.00
	0.74	0.39042	0.40485	1.00
	0.75	0.49150	0.49930	0.99
	0.76	0.60339	0.60462	0.98
	0.77	0.72676	0.72159	0.97
0.9	0.0089	0.0085215	0.0085335	1.21
	0.0266	0.023298	0.023314	1.21
	0.0444	0.035426	0.035204	1.21
	0.66	0.22651	0.23150	1.04
	0.67	0.27310	0.26561	1.02
	0.68	0.32557	0.31686	1.02
	0.69	0.38442	0.39418	1.02
	0.70	0.45013	0.45378	1.01
	0.71	0.52323	0.52059	1.00
	0.72	0.60426	0.59524	0.99
	0.73	0.69378	0.70840	0.99
	0.74	0.79237	0.80179	0.98
	0.75	0.90064	0.90488	0.97
	0.76	1.0192	1.0184	0.96
	0.77	1.1487	1.1430	0.95
	0.78	1.2897	1.2795	0.94
	0.79	1.4430	1.4285	0.93
	0.80	1.6092	1.5909	0.92
1.1	0.10	0.072704	0.072188	1.21
	0.20	0.10767	0.10402	1.21
	0.30	0.12933	0.12662	1.21
	0.40	0.15870	0.15817	1.17
	0.50	0.22913	0.22578	1.11
	0.60	0.42822	0.42561	1.05
	0.70	0.95659	0.96017	0.98
	0.80	2.1813	2.2087	0.90

1.3	0.10	0.081073	0.081195	1.21
	0.20	0.13714	0.13712	1.21
	0.30	0.19052	0.19227	1.21
	0.40	0.26573	0.26486	1.15
	0.50	0.40043	0.39672	1.09
	0.60	0.67766	0.67802	1.03
	0.70	1.2749	1.2694	0.95
	0.80	2.5139	2.5300	0.87
1.5	0.10	0.086896	0.087138	1.21
	0.20	0.15812	0.15919	1.21
	0.30	0.23454	0.23840	1.21
	0.40	0.34233	0.34622	1.15
	0.50	0.52091	0.52227	1.08
	0.60	0.84869	0.85071	1.01
	0.70	1.4845	1.4836	0.93
	0.80	2.7136	2.7134	0.84

B. Results of MD simulations for adsorption

All results of the molecular dynamics (MD) simulations for the vapor and liquid phase are given in Table 2 and 3, respectively.

Table S2: Bulk fluid density $\rho_{\mathrm{f}}^{*\mathrm{b}}$, bulk fluid pressure p_{f}^{*}, and surface excess Γ^{*} for the vapor phase adsorption simulations with changing wall potential, temperature T^{*}, and surface energy $\varepsilon_{\mathrm{sf}}^{*}$. The number in parenthesis indicates the statistical uncertainty in the last decimal digits.

wall potential	T^{*}/T_{c}^{*}	$\varepsilon_{\mathrm{sf}}^{*}$	$\rho_{\mathrm{f}}^{*\mathrm{b}}$	p_{f}^{*}	Γ^{*}
LJ-10-4-3	0.8	0.514	0.00925(10)	0.00752(27)	0.0346(46)
			0.02095(38)	0.0160(8)	0.099(17)
			0.0305(6)	0.0220(9)	0.187(32)
			0.0370(10)	0.0251(14)	0.537(45)
LJTS-10-4-3	0.8	0.3	0.01017(5)	0.0083(5)	0.0102(34)
			0.01688(10)	0.01305(46)	0.017(6)
			0.0226(14)	0.0172(10)	0.022(9)
			0.0333(5)	0.0236(10)	0.039(21)
			0.04204(33)	0.0278(21)	0.050(15)
			0.05075(43)	0.0313(16)	0.074(21)
		0.514	0.00941(5)	0.00765(33)	0.0271(25)
			0.01621(15)	0.0127(7)	0.050(9)
			0.02157(12)	0.0164(8)	0.0706(8)
			0.0315(7)	0.0223(12)	0.126(31)
			0.03711(44)	0.0257(14)	0.179(21)
			0.0419(10)	0.0278(12)	0.24(6)
		0.75	0.00897(13)	0.00735(25)	0.069(6)
			0.01454(35)	0.0115(6)	0.132(19)
			0.01887(49)	0.0146(7)	0.203(26)
			0.0259(6)	0.0193(5)	0.402(33)
			0.0281(9)	0.0206(10)	0.531(45)
			0.0298(10)	0.0216(11)	0.649(49)
			0.0305(10)	0.0219(14)	0.74(5)
			0.0306(10)	0.0219(13)	0.792(48)
			0.0317(10)	0.0225(14)	0.86(5)
			0.0323(8)	0.0229(15)	0.979(39)
			0.0338(7)	0.0235(8)	1.320(35)
			0.0338(11)	0.0236(7)	1.72(6)
		2.0	0.00053(10)	0.00045(8)	0.4890(49)
			0.00242(11)	0.00207(14)	0.735(6)
			0.00553(19)	0.00458(10)	0.867(10)
			0.01117(29)	0.00898(40)	1.133(16)
			0.0156(8)	0.0123(7)	1.354(42)
			0.0201(9)	0.01539(35)	1.582(48)
			0.0239(15)	0.0178(9)	1.81(9)
			0.0273(9)	0.0199(12)	2.037(46)

	1.1	0.514	0.01006(7)	0.01169(33)	0.0145(41)
			0.03299(29)	0.0358(7)	0.050(16)
			0.05053(27)	0.0508(31)	0.074(16)
			0.0664(6)	0.0638(36)	0.101(35)
			0.08285(46)	0.0767(38)	0.124(11)
			0.1062(9)	0.0913(21)	0.15(6)
			0.1258(10)	0.1000(42)	0.193(39)
			0.1489(19)	0.112(7)	0.23(8)
			0.1698(14)	0.1178(39)	0.20(9)
LJ-9-3	0.8	0.514	0.00963(5)	0.00779(28)	0.0152(26)
			0.02213(8)	0.0166(5)	0.0405(44)
			0.03294(16)	0.0232(14)	0.064(9)
			0.0456(9)	0.0296(22)	0.109(45)
LJTS-9-3	0.8	0.514	0.00970(6)	0.00784(37)	0.0117(25)
			0.02240(27)	0.0168(8)	0.028(11)
			0.03334(35)	0.0235(8)	0.044(16)
			0.04654(41)	0.0300(19)	0.066(20)

Table S3: Bulk fluid density $\rho_{\mathrm{f}}^{*\mathrm{b}}$ and bulk fluid pressure p_{f}^{*} for liquid phase adsorption simulations with changing wall potential, temperature T^{*}, and constant surface energy $\varepsilon_{\mathrm{sf}}^{*} = 0.514$. The number in parenthesis indicates the statistical uncertainty in the last decimal digits.

wall potential	T^{*}/T_{c}^{*}	$\rho_{\mathrm{f}}^{*\mathrm{b}}$	p_{f}^{*}	Γ^{*}
LJ-10-4-3	0.8	0.7212(10)	0.190(25)	0.079(43)
		0.7733(6)	0.648(37)	0.096(22)
		0.81324(23)	1.189(38)	0.106(11)
LJTS-10-4-3	0.7	0.7689(13)	0.108(20)	0.061(41)
		0.7785(16)	0.198(37)	0.073(43)
		0.8216(11)	0.72(8)	0.108(28)
	0.8	0.7030(38)	0.086(20)	0.02(5)
		0.7218(11)	0.194(32)	0.042(47)
		0.7474(10)	0.394(38)	0.064(40)
		0.7685(8)	0.60(7)	0.082(31)
		0.7738(5)	0.651(42)	0.071(12)
		0.8136(6)	1.195(49)	0.090(18)
	0.9	0.6933(13)	0.393(35)	0.050(48)
		0.7476(8)	0.841(42)	0.081(42)
		0.7704(7)	1.12(8)	0.095(42)
	1.5	0.68004(31)	2.18(7)	0.087(37)
		0.7386(5)	3.08(7)	0.103(28)
		0.7614(7)	3.52(12)	0.113(35)
LJ-9-3	0.8	0.7218(11)	0.193(29)	-0.035(38)
		0.7729(6)	0.644(41)	0.032(16)
		0.8123(5)	1.174(40)	0.066(19)
LJTS-9-3	0.8	0.7225(10)	0.196(26)	-0.077(29)
		0.7733(5)	0.648(43)	0.013(16)
		0.81263(46)	1.179(36)	0.051(15)

C. Additional Figures

In the following subsections, further figures regarding the radial distribution function and density profiles are shown.

C.1 Radial distribution functions at $T^*/T_c^* = 0.8$ and 1.1

A comparison between the simulated (with Monte Carlo (MC) simulations) and DFT predicted $g(r^*)$ for $T^*/T_c^* = 0.8$ and 1.5 is shown in Figure 1.

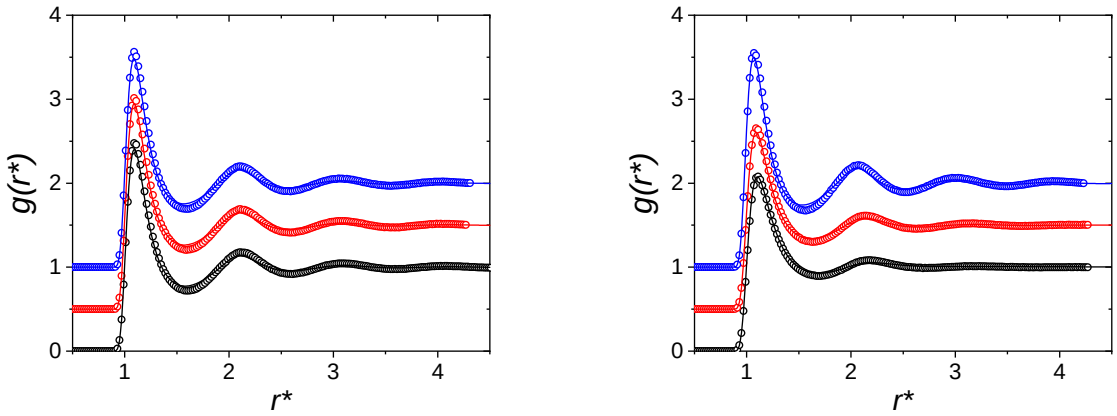

(a) (b)

Figure S1: Radial distribution functions $g(r^*)$ at different temperatures from NVT MC simulations (symbols) and DFT1 (solid lines) for (a) $T^*/T_c^* = 0.8$ with $\rho_{\mathrm{f}}^{*\mathrm{b}}$ equal to 0.69 (black), 0.71 (red), and 0.73 (blue); (b) $T^*/T_c^* = 1.1$ with $\rho_{\mathrm{f}}^{*\mathrm{b}}$ equal to 0.40 (black), 0.60 (red), and 0.80 (blue). For reasons of clarity, the radial distribution functions are shifted by $g(r^*) = 0.5$ with increasing $\rho_{\mathrm{f}}^{*\mathrm{b}}$.

C.2 Liquid density profiles on a LJTS-10-4-3 surface at $T^*/T_c^* = 0.8$ and 0.9

Predictions of liquid density profiles with DFT1, the approach with the surface tension fitted $\varphi = 1.21$ (DFT2), and density gradient theory (DGT) are compared to MD simulation results for one external potential in Figure 2.

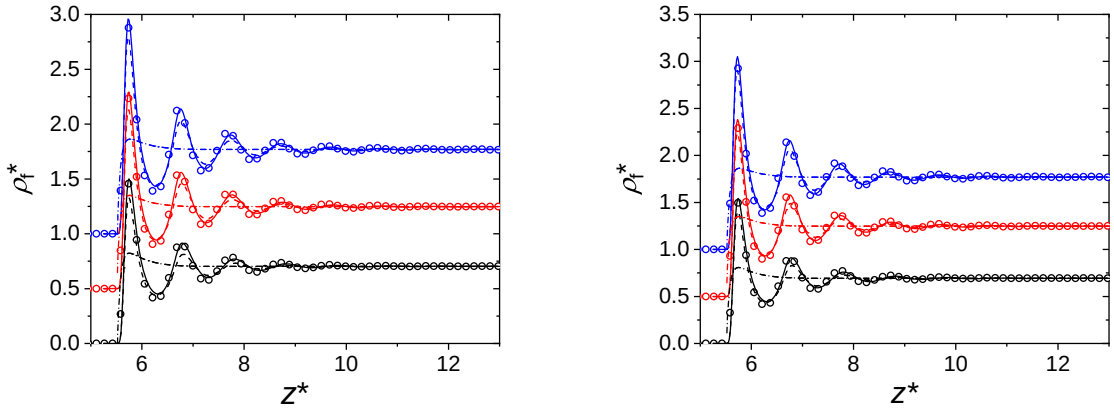

(a) (b)

Figure S2: Comparison of adsorbed liquid density profiles on a LJTS-10-4-3 surface predicted by DFT1 (solid lines), DFT2 (dashed lines), and DGT (dash dotted lines) with MD simulations (symbols) at a fixed surface energy ($\varepsilon_{sf}^* = 0.514$) and (a) $T^*/T_c^* = 0.8$ for $\rho_f^{*b} = 0.77$ (black), 0.78 (red), and 0.82 (blue); (b) $T^*/T_c^* = 0.9$ for $\rho_f^{*b} = 0.70$ (black), 0.75 (red), and 0.77 (blue). For reasons of clarity, the density profiles are shifted by $\rho_f^* = 0.5$ with increasing ρ_f^{*b}.

C.3 Vapor density profiles for different external potentials at $T^*/T_c^* = 0.8$

A comparison of vapor density profiles predicted by DFT1/DFT2 and DGT with MD simulation results for all different external potentials studied in this work is shown in Figure 3. The bulk densities are approximately the same for all potentials.

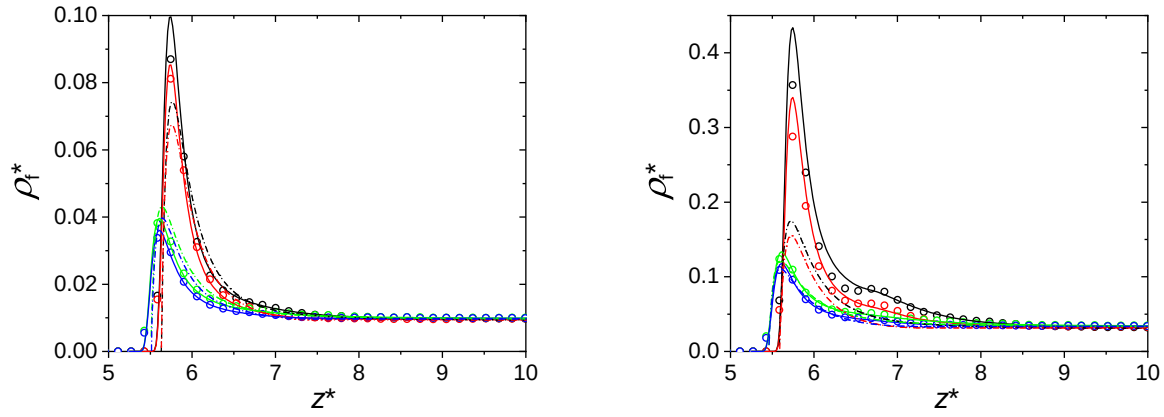

(a) (b)

Figure S3: Comparison of adsorbed gas density profiles predicted by DFT1/DFT2 (solid lines) and DGT (dashed lines) with MD simulations (symbols) for different external potential forms for the surface energy $\varepsilon_{sf}^* = 0.514$ and $T^*/T_c^* = 0.8$. Bulk gas densities are approximately the same in each graph with (a) LJ-10-4-3 and $\rho_f^{*b} = 0.00925$ (black), LJTS-10-4-3 and $\rho_f^{*b} = 0.00941$ (red), LJ-9-3 and $\rho_f^{*b} = 0.00963$ (green), LJTS-9-3 and $\rho_f^{*b} = 0.00970$ (blue) (b) LJ-10-4-3 and $\rho_f^{*b} = 0.0305$ (black), LJTS-10-4-3 and $\rho_f^{*b} = 0.0315$ (red), LJ-9-3 and $\rho_f^{*b} = 0.03294$ (green), LJTS-9-3 and $\rho_f^{*b} = 0.03334$ (blue).

C.4 Liquid density profiles for different external potentials at $T^*/T_c^* = 0.8$

A comparison of liquid density profiles predicted by DFT1 and DFT2 with MD simulation results for all external potentials studied in this work is shown in Figure 4. The bulk densities are approximately the same for all potentials.

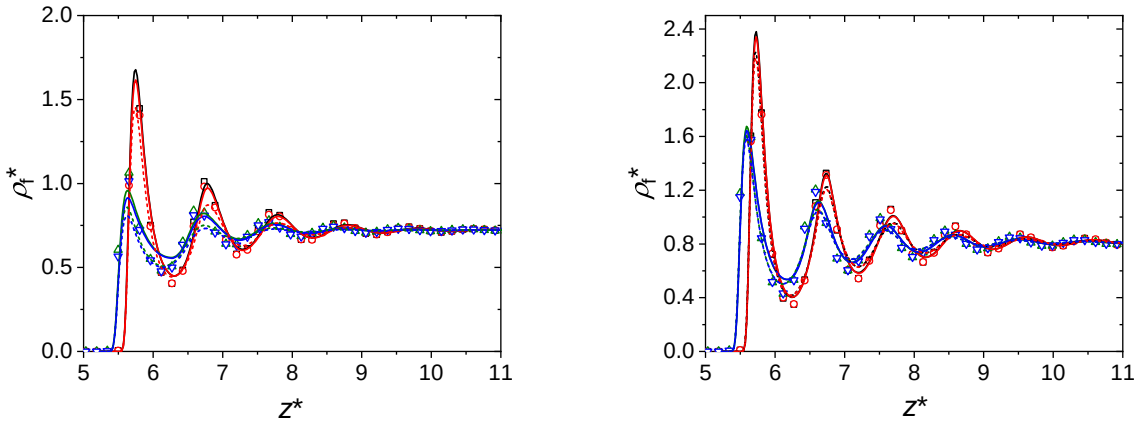

(a) (b)

Figure S4: Comparison of adsorbed liquid density profiles predicted by DFT1 (solid lines), DFT2 (dashed lines) with MD simulations (symbols) for different external potential forms (LJ-10-4-3 (black), LJTS-10-4-3 (red), LJ-9-3 (green), and LJTS-9-3 (blue)) at a fixed surface energy ($\varepsilon_{\rm sf}^* = 0.514$) and $T^*/T_c^* = 0.8$. Bulk densities are approximately the same in each graph with (a) $\rho_{\rm f}^{*\rm b} \approx 0.72$; (b) $\rho_{\rm f}^{*\rm b} \approx 0.81$.

D. LJTS-2.5 σ_{f} phase diagram

The simulation points at gaseous states, including stable and metastable, are shown on the LJTS-2.5 σ_{f} fluid phase diagram predicted by PeTS EOS.

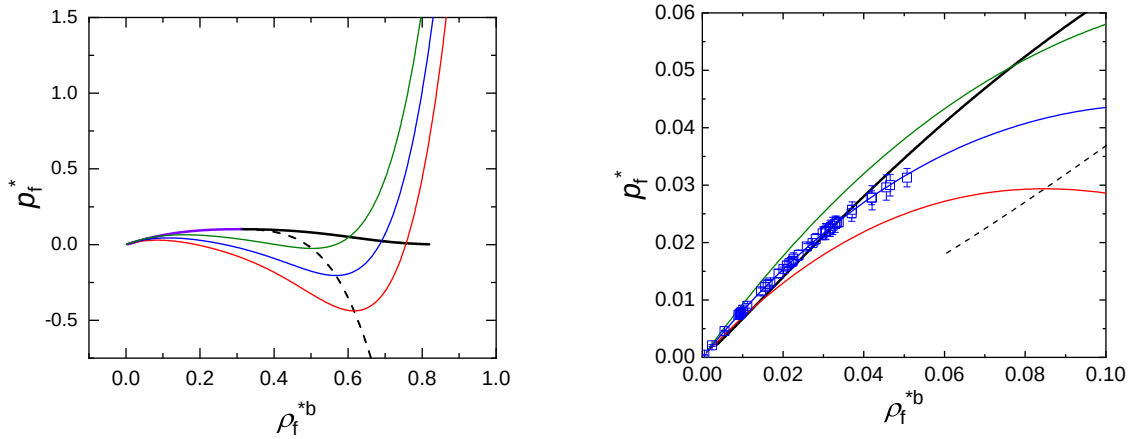

(a) (b)

Figure S5: Bulk pressure versus density for LJTS-2.5 σ_{f} fluid calculated with PeTS EOS for $T^*/T_c^* = 0.7$(red), 0.8 (blue) and 0.9(green). The binodal is shown as a purple line for vapor side and black line for liquid side. The spinodal is shown as a black dashed line. (a) Phase diagram of the LJTS-2.5 σ_{f} calculated with the PeTS EOS. (b) Bulk pressure versus density for vapor side. The bulk pressures of the adsorption simulations are shown as symbols for $T^*/T_c^* = 0.8$.